Theor Chem Acc (2006) 116: 598–607
DOI 10.1007/s00214-006-0105-5

REGULAR ARTICLE

Michèle Leduc · Jacques Vigué

Interplay between theoretical quantum chemistry and cold atom experiments

Received: 24 November 2004 / Accepted: 28 February 2005 / Published online: 15 June 2006

Abstract In this paper, we briefly summarize the new information which have been deduced on the atom–atom interaction from cold atom experiments. These information are quite unusual and very interesting. Their interpretation is considerably simplified if high quality quantum chemistry calculations are available. After an overview of the domain, we discuss in detail the experiments performed with metastable helium atom, thus showing the variety of new data obtained in this case and the importance of quantum chemistry calculations for their interpretation.

1 Introduction

The development of cold atom physics has induced an unexpected renewal of the field of the atom–atom interaction, in particular at long distances. New types of information have been obtained, which, like the atom–atom scattering length, are very sensitive to the properties of the interatomic potentials. This large sensitivity makes that quantum chemistry calculations must reach an unusual degree of accuracy if one wants to be fully predictive. Such accuracy has only been achieved for few-electron systems like metastable helium dimer (which is discussed below in great detail) or LiH [1,2]. There are other quantities, such as photoassociation rates or fine structure relaxation rates, which are experimentally observed with cold atoms and which are less sensitive to the molecular potentials. To fully understand these experiments and to predict their outcome with new atoms which have not been studied up to now, high quality quantum chemistry calculations are needed and they are very interesting as these experiments explore new domains of the interatomic potentials.

In the very low energy regime, interatomic collisions can be described by only one quantity, the s wave scattering length a. This quantity governs the physics around Bose–Einstein condensation (BEC): its value plays very important roles in the kinetics of the evaporative cooling process needed to prepare the condensation, in the stability and shape of the condensate, and in its expansion regime. It has been shown that the scattering length can be modified by external fields, such as magnetic fields or laser fields, with very rapid variations near Feshbach resonances. An accurate knowledge of a governs the feasibility of most BEC studies and of related works with degenerate Fermi gases.

Another new domain opened up by the cold atom experiments is the photoassociation spectra with very high resolution. Photoassociation corresponds to a free-to-bound transition and the excitation to a given excited state gives a spectrum with a width comparable to $k_B T$, where T is the temperature of the gas. At ordinary temperature, a photoassociation spectrum is unresolved but when the temperature of the gas is very low, below 1 mK, such an experiment provides a spectrum with narrow lines. Numerous photoassociation spectra have been recorded, giving access to high accuracy information on the very long-range part of molecular potentials.

Very exotic molecular states have also been studied, through experiments involving metastable electronic states, usually with rare gases. The case of helium 2^3S_1 state is particularly striking: molecules with about 40 eV of internal energy can be produced and long-lived states have been observed. Due to the presence of only four electrons, very sophisticated ab initio calculations are possible. This is at variance with the case of alkali molecules for which an effective core potential is the basis of almost all the high quality ab initio works: although aiming a slightly less good accuracy, these calculations are extremely useful too.

In this paper, we present some striking results concerning atom–atom interactions, deduced from experiments involving

M. Leduc (✉)
Laboratoire Kastler-Brossel, CNRS-UMR 8552,
Ecole Normale Supérieure 24, rue Lhomond,
75 231 Paris Cedex 05, France
E-mail: leduc@lkb.ens.fr

J. Vigué
Laboratoire Collisions Agrégats Réactivité – IRSAMC,
Université Paul Sabatier and CNRS UMR 5589,
118, Route de Narbonne, 31062 Toulouse Cedex, France
E-mail: jacques.vigue@irsamc.ups-tlse.fr

cold atomic gases. We show how the experimental results and the quantum chemistry calculations have been supporting each other. In a first part, we discuss the connection between ultra-cold atomic gases and molecular physics and, in a second part, we illustrate this discussion by various results concerning the helium dimers produced by the interaction of metastable helium atoms.

2 Molecular physics connected to ultra-cold atom experiments

2.1 Introduction

Laser cooling is very efficient to produce atomic gases with temperatures T down to a few microkelvins and atomic densities n_{at} in the 10^9–$10^{11}\,\mathrm{cm}^{-3}$ range. In the microkelvin temperature range, such densities are too low to reach the domain of the quantum collective effects, such as Bose–Einstein condensation and Fermi degeneracy. These effects appear when the thermal de Broglie wavelength $\Lambda = (2\pi\hbar^2/mk_BT)^{1/2}$ verifies $n_{at}\Lambda^3 \sim 1$. When $T \approx 1\,\mu\mathrm{K}$, for an atomic species of mass number A, the needed density is close to $n_{at} \sim 2{\times}10^{11}{\times}A^{3/2}\,\mathrm{cm}^{-3}$. Evaporative cooling in a magnetic or laser trap, briefly described below, permits to reach the degeneracy regime. However, much spectroscopy has been done in cold and dense gases, which are close to but not in the quantum degeneracy regime.

2.2 The atom–atom scattering length and its importance for Bose–Einstein condensation

For identical bosons in the same internal state, at very low energies, the collisions are in the quantum threshold regime, where only the s-wave plays a role and the collision cross section is given by $\sigma = 8\pi a^2$. In this expression, a is the scattering length, defined by $a = -\lim \tan \delta_0/k$ when $k \to 0$. Here δ_0 is the s-wave collisional phase shift and k is the wavenumber describing the relative motion of the two atoms.

To increase the density while keeping the gas very cold, the technique of general use is evaporative cooling in a magnetic or laser trap. The kinetic theory of this method was developed by Ketterle [3] and by Luiten et al. [4]. The atoms initially confined in a magnetic trap at a temperature of the order of 1 mK have their energy redistributed by elastic collisions. A few atoms acquiring energies larger than the trap depth are expelled from the trap. This significantly reduces the mean energy of the trap ensemble while only a relatively small number of atoms is lost. In forced evaporative cooling, the trap depth is gradually lowered; the cooling increases the density and thus the elastic collision rate, accelerating the evaporation: this is called the run-away regime. In this process, the key parameters are the various collision cross-sections: the elastic cross-section must be large enough for an efficient evaporative cooling, while the cross section for inelastic processes must be small because these processes reduce the number of atoms. The feasibility of evaporative cooling is therefore strongly dependent on the value of a.

When a Bose–Einstein condensate is formed in a trap, it is usually submitted to some perturbations and after some evolution, one wants to know its final state. This is done by imaging the condensate after suppressing the trapping potential and letting the condensate expand freely. This expansion phase is necessary because the initial size is usually too small for imaging and also because the final shape gives an image of the momentum distribution in the condensate. This last property is valid if the expansion is collisionless; however large condensates are close to the hydrodynamic regime, with a mean free path smaller than at least one dimension of the condensate. As a consequence, the expansion is also sensitive to the value of the collision cross-section.

The simplest description of a dilute Bose–Einstein condensate is obtained by neglecting the atom–atom interactions, but this is too crude an approximation which does not account for the observed results. The next approximation, which is most commonly used, consists in replacing the exact atom–atom interaction potential by a zero-range pseudopotential (following a procedure introduced by Fermi) and to establish the Gross–Pitaïevski equation. This equation, which describes well an almost pure condensate with a mean number of atoms N_0 in an external potential U, is a modified Schrödinger equation with a non linear term proportional to the density:

$$i\hbar\frac{\partial\psi}{\partial t} = \left[-\frac{\hbar^2}{2m}\Delta + U + N_0 g|\psi|^2\right]\psi \tag{1}$$

Here m is the atomic mass and the coefficient g of the non-linear term is related to the scattering length a by $g = 4\pi\hbar^2 a/m$. An important point is that if a is positive (respectively negative), the atoms behave as if their effective interaction is repulsive (respectively attractive) and Bose-Einstein condensates are stable for all N_0 values if $a > 0$ and only for small N_0 values if $a < 0$.

The scattering length is very sensitive to the molecular potential, so that very few atom–atom scattering lengths were known twenty years ago, an exception being the case of H_2 singlet and triplet states (see for example [5]). This very large sensitivity is related to Levinson theorem which states that the scattering length is infinite when the molecular potential holds a zero-energy bound state. More precisely, if we imagine that we could slowly increase the potential depth, the scattering length which is infinite and positive when the potential just holds a new bound states, decreases till it becomes infinite and negative just before the apparition of a new bound state. The value of the scattering length can be quantitatively related to the position of the highest vibrational level by an analytic formula due to Gribakin and Flambaum [6]:

$$a = \bar{a}\left[1 - \tan\left(\frac{\pi}{n-2}\right)\tan\left(\phi - \frac{\pi}{2(n-2)}\right)\right] \tag{2}$$

Here n is the exponent of the leading term of the the potential at long range, which is assumed to be attractive,

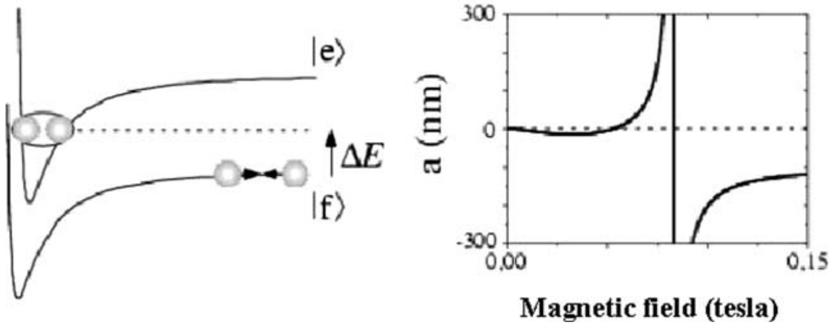

Fig. 1 Principle of the Feshbach resonance. One shifts a molecular bound state |e⟩ with a magnetic field, as shown in the left part of the figure. When the energy ΔE of this state becomes resonant with that of the pair of atoms, the scattering length diverges. To the right: scattering length of ^{6}Li atoms of opposite signs as a function of the magnetic field, in Tesla. The Feshbach resonance is localized close to 0.0834 T

equal $-C_n/r^n$, and ϕ is the semiclassical phase calculated for zero energy. Finally, $\bar{a}$ is a mean scattering length which depends of C_n and of the reduced mass. Most molecular potentials hold several tens of vibrational levels and the work of Leroy and Bernstein [8] and of Stwalley [9] has enabled a very accurate description of the series of vibrational levels converging toward the dissociation limit. When the knowledge of an accurate value of the scattering length was understood as very important for ultra-cold atom experiments, the available spectroscopic data appeared not to be accurate enough to predict the value of the atom–atom scattering length: the uncertainty on the number of vibrational bound states was usually comparable to 1 corresponding to an uncertainty equal to π on the phase ϕ appearing in the Gribakin and Flambaum formula, so that the scattering length could take any value from $-\infty$ to $+\infty$! Many efforts have been done to improve the accuracy on the molecular data by traditional molecular spectroscopy and these results have been complemented by experiments using cold atomic gases, in order to determine accurately these scattering lengths. We will describe these efforts in the case of $\mathrm{He}_2\ {}^5\Sigma_g^+$ state in the last chapters.

Tuning the value of the scattering length is of great practical importance for the studies of BEC. It appears even more important with Fermi ultra-cold gases, but we will not discuss this question here. To explain how such a tuning is possible, we will take the examples of the alkali atoms which are commonly used. These atoms have an electronic spin $S = 1/2$ in their ground state and they have also a non-zero nuclear spin (for most of the isotopes). There are two interaction potential curves corresponding to a singlet and a triplet molecular state converging toward the same dissociation limit. In the presence of a non-zero magnetic field, the triplet state dissociation limit splits in three different limits due to the Zeeman effect and some bound triplet or singlet states corresponding to an upper dissociation limit are imbedded in the continuum of the lower limits. These discrete states are coupled to the continuum and the scattering length associated to one of these potentials present resonant variations, which are called Feshbach resonances, when a discrete state crosses the dissociation limit [10,11]. In favorable cases, like in cesium-cesium interaction, many different resonances can be observed and theoretically explained with an excellent accuracy [12]. The Feshbach resonances can be used to tune the scattering length a [13]. The principle of the method is illustrated in Fig. 1, which shows the abrupt divergence of a for a given value of the magnetic field. Finally, rather than using a static magnetic field, it has been suggested to use a other coupling terms (RF fields [14], static electric field [15], laser fields [16]) to induce a Feshbach resonance.

2.3 Other collision processes

Many other collision processes are important with cold atoms. These processes usually involve effects at short and long range simultaneously: due either to the very low initial kinetic energy or to a laser excitation process, the collision is very sensitive to the long range part of the potential in its entrance channel, while, for instance, an inelastic process occurs at some potential curve crossing at short range.

The simplest case, which was probably the first to be studied, is the case of laser induced collisions in traps, detected through the loss of atoms. An atom pair is excited at long range by a laser beam which is quasi-resonant with the atomic transition and the excited atomic pair is attracted by the upper state potential (assumed here to be attractive) toward short internuclear distances. Following Gallagher and Pritchard [17], two different inelastic events may occur :

- A transition between electronic states connected to different atomic fine structure states; the atom pair shares an energy equal to the fine structure splitting.
- The emission of a fluorescence photon with a frequency different from the excitation frequency.

In both cases, the energy gained by the atoms is in general sufficient to authorize the escape of the atom pair out of the trap. The competition between these two processes was studied through the alkali dimers by [18] Julienne and one of us. Their model was used many times, with some further developments. In the calculation done in our paper, we needed molecular potentials for the alkali dimers and we had to connect the long-range r^{-3} potentials corresponding to the $^2S + {}^2P$ dissociation limit, with short range potentials calculated by Krauss and Stevens [19]. Finally, as the fine structure was neglected in these calculations, we used experimental determinations of the coupling between singlet and triplet molecular potentials to calculate the rate of fine structure relaxation collisions for cold atom applications.

Some other inelastic processes are very important:

- An example is the relaxation of spin polarization in ultracold gases. In magnetic traps, only the so-called low field seekers can be trapped. These Zeeman sub-levels have an energy which increases with the magnetic field and obviously there must be other Zeeman sub-levels with opposite M-values, whose energy decreases with the magnetic field (they are high field seekers) and which are at a lower energy. Relaxation toward these levels is usually forbidden to some degree by an approximate conservation law and for an efficient trap, the corresponding cross-section must be considerably lower than the elastic cross-section: if an atom is transformed in a high field seeker by relaxation, it is immediately expelled from the magnetic trap. The ratio of these two cross sections (elastic collision and spin relaxation collision) governs the feasibility of evaporative cooling in a magnetic trap.
- A very important application of cold atoms is the development of new atomic clocks with an atomic fountain. Although the atomic density is quite low in these clocks, the collisions induce a shift of the frequency which is quite substantial for cesium [20] and considerably smaller for rubidium [21]. The calculation of these frequency shifts is possible thanks to a high accuracy knowledge of the relevant interaction potentials.

2.4 The photoassociation spectroscopy method

Photoassociation corresponds to a free to bound transition. At ordinary temperature, the energy width of the occupied levels of the continuum, of the order of $k_B T$, is large and the spectrum does not present narrow lines. For a temperature $T \sim 100\,\mu\mathrm{K}$, the energy width of the occupied levels of the continuum is usually lower than the width of the excited state (due to its decay processes) and then, photoassociation provides very high resolution spectra, with very narrow lines, if the broadening effects due to laser linewidth and/or to laser saturation are negligible.

Obviously, many other techniques give high accuracy information on molecular potential curves and one may quote, for instance, photoelectron spectroscopy which has recently provided impressive results, such as an almost complete description of the six electronic states of Ar_2^+ molecular ion [22].

Because, most of the time, the interatomic distance in a colliding atom pair is very large (simply for a phase space argument), a photoassociation spectrum gives an easy access to the very long-range part of molecular potentials, a region which is very difficult to study by traditional technique. The reason is that the Franck-Condon principle forbids the excitation of molecular states which are at very long range in a single step from the lowest vibrational state of the molecule. Some clever experiments with two-step excitation have been made [23] to study very long-range molecular levels, but most of the data on these levels is due to photoassociation with cold atomic gases.

A spectacular case was the first observation in 1994 by Heinzen and co-workers [24] of purely long range states which were predicted in 1978 by Stwalley et al. [25]: these electronic states have a very shallow potential well located at a very large internuclear distance, resulting from an avoided crossings of two states converging to different fine structure components of an atomic state. In dimers made of two identical atoms, the interaction between one excited and one ground state atom is the resonant dipole–dipole interaction proportional to C_3/r^3 at large interatomic distance r, if one neglects relativistic retardation effects.

Photoassociation spectroscopy gives access to the C_3 coefficient, which is directly related to the matrix element of the atomic dipole between the ground and excited states. The spectroscopy can be so accurate that it gives the most accurate values of the ^2S–^2P dipole moments for the alkali atoms: we quote the first works [26,27] and similar results are now available for several other atoms. Another striking point concerning these experiments is that the data analysis must include relativistic retardation effects. Because of these effects, the leading term of the long-range potential differs substantially from the simple non-retarded form C_3/r^3 term when the internuclear distance r is comparable to $\lambda/2\pi$ (where λ is the wavelength of the atomic resonance transition) and the resulting corrections on the vibrational level energies are easily detected.

Finally, photoassociation spectra provides two methods for determining accurate and precise values of scattering lengths:

- In the first method, photoassociation is used to probe the position of the nodes of the radial wave function describing the atomic pair colliding at very low energy. The positions of these nodes are reflected in the intensities of the transitions observed in the photoassociation spectra, through the Franck–Condon factors: each minimum reveals the existence of a node and its position is deduced from the spectroscopy of the excited state. From the position of the node, one can easily deduce the sign and magnitude of the scattering length [28].
- The second method uses a two-photon photoassociation Raman process. In such an experiment, the colliding atom pair is excited by the first photon and de-excited by the second photon, producing the molecule in the highest vibrational level of the ground molecular state. The binding energy of the highest level is deduced from the frequency difference between the two lasers and the scattering length is directly related to the energy of the highest vibrational level. This experiment has even been performed in a Bose–Einstein condensate, giving extremely narrow lines [29].

We will not try to review all the works on photoassociation, as very many papers have appeared, including several reviews [30–32]. We may simply point out that such experiments have already been carried with all the alkalis, with hydrogen, metastable helium, calcium, ytterbium, and the list extends regularly, for instance with heteronuclear alkalis.

3 Ultracold metastable helium gas: a rich system for theoretical investigations

3.1 Metastable helium is an interesting case

Metastable helium in the 2^3S_1 state has been the subject of many experimental investigations at cold and ultracold temperatures since the appearance of laser cooling and of the first magneto-optical traps. The interest of such a simple two electron atom, as compared to alkali atoms discussed in the previous chapters, is that ab initio calculations of interaction potentials are possible, even if still not with sufficient precision for the experiments. The main feature of metastable helium atom in the 2^3S_1 state is that it carries a very large internal energy of 20 eV (see Fig. 2). However, in most cases, it can be considered as a ground state atom because its intrinsic lifetime is very long (8, 000 s). A drawback of dealing with such an excited atom is that it has a strong probability to be destroyed by ionizing collisions of the Penning type when it collides with another metastable atom, giving rise to a He^+ or He_2^+ ion [33,34]. Fortunately, this Penning ionization rate is strongly inhibited by spin polarization of the two atoms, as a consequence of the Wigner spin conservation law during collisions. This inhibition, by more than 4 orders of magnitude, was initially predicted theoretically [35,36]. It was fully confirmed experimentally by the possibility of trapping metastable helium atoms at large densities. It was the condition which made it possible to reach Bose Einstein condensation.

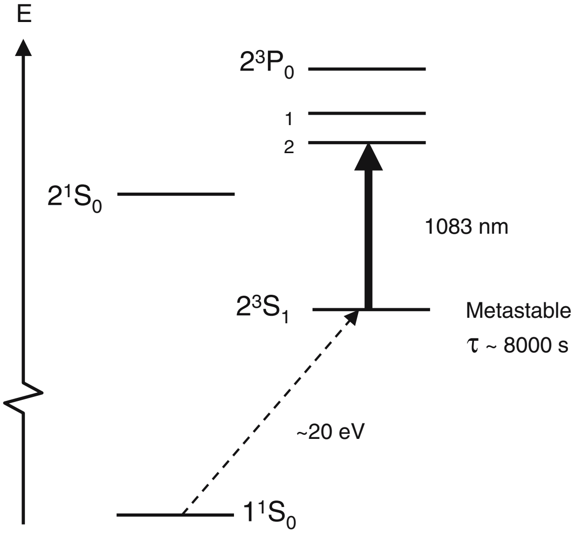

Fig. 2 Scheme of the relevant levels of the helium atom. The 2^3S_1 metastable state is long-lived and carries a large internal energy of 20 eV. In cold atom experiments, this metastable helium atom is manipulated by laser light tuned to the 2^3S_1–2^3P transition at 1,083 nm

The interest for laser cooling experiments with metastable helium still rose when Bose–Einstein condensation of this atom was achieved in 2001 by two groups in France [37,38]. This result stimulated the work of theoreticians to investigate the collision properties of the cold metastable helium gas and to calculate the interaction between two spin polarized metastable atoms in the quintet $He_2\ {}^5\Sigma_g^+$ molecular potential. As mentioned earlier in this article, for temperatures in the microkelvin range, the scattering between the particles is ruled by the s-wave scattering length, the value of which is very much in demand to interpret the dynamical properties of the ultracold gas and of the condensate. In this section, we first briefly review the theoretical attempts for ab initio calculation of the interaction potentials. We then describe the various experimental methods which have been used to measure the value of a after that BEC was achieved. The methods are quite dissimilar: expansion of the condensate, oscillation modes in the hydrodynamical regime, inelastic collision rates through ion detection, and finally photoassociation spectroscopy.

3.2 Calculating the s-wave scattering length

The first accurate calculation of the interaction $He_2\ {}^5\Sigma_g^+$ potential between two spin polarized 2^3S_1 metastable helium atoms was made by Stärck and Meyer in 1994 [39] and more elaborate calculations have been made by Gadéa et al. in 2002 [40] and in 2004 [41].

In the Stärck and Meyer paper [39], the ${}^5\Sigma_g^+$ van der Waals potential curve of the two interacting He (2^3S_1) atoms has been determined from the multi-reference configurations with an estimated accuracy of about 1% of the well depth equal to 1,045 cm^{-1} and corresponding to an internuclear distance $r_e = 7.34\ a_0$. The calculated well depth is considerably deeper than in previous calculations and this well supports 15 bound vibrational states, the highest one ($v = 14$) being rather close to the dissociation limit. The limited accuracy of this potential introduces uncertainties in the position of the highest vibrational level, and consequently in the value of the scattering length a associated with the quintet potential, which controls the collision dynamics of spin polarized metastable helium atoms. In an article published in 2001, Leo et al. [42] calculated the possible range of values for a directly associated with a hybrid molecular potential: for the long range part, they used a $-C_n/r^n$ multipole expansion taken from [43] and for the short range part, they used the Stärck and Meyer's results. They varied the short range potentials by ±2.5% to obtain an estimate of the range of possible a values. In agreement with previous estimates, they obtain $a \approx 8.3$ nm and, as predicted by Eq. 2, they find that a changes enormously when they vary the potential, with a divergence for a 1.8% decrease of the well depth, beyond which a becomes negative (see Fig. 3 of [42]). Such a divergence corresponds to the case when the highest vibrational level $v = 14$ reaches the dissociation limit and disappears for a larger change of the potential (which then hold 14 and no longer 15 vibrational levels. These results illustrate the need

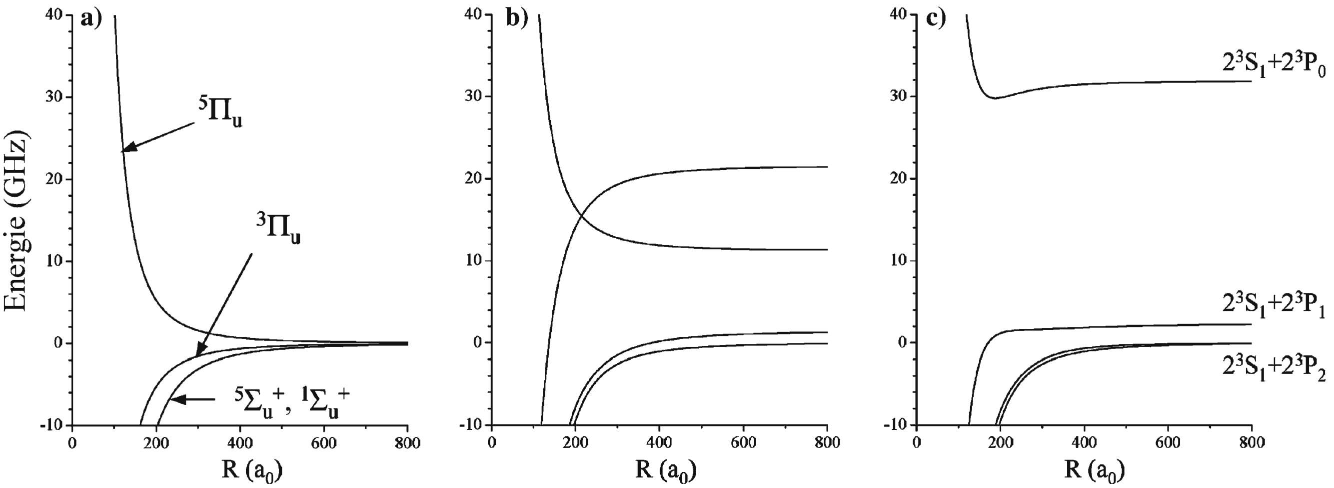

Fig. 3 Physical origin of the purely long-range interaction potentials between two helium atoms in the ^2S and ^2P states. The figure shows the joint effect of the dipole–dipole interaction and of the fine structure coupling on the 0_u^+ subspace. Energies are given in GHz, internuclear distances in atomic units. **a** In this part the fine structure coupling is neglected. The potential curves are the eigenvalues of the dipole-dipole interaction corresponding to the four Hund's case a eigenstates. **b** In this part the fine structure terms are partially introduced, neglecting the couplings between the attractive and the repulsive states. A level crossing appears. **c** In this part all fine structure terms are included, corresponding to a coupling between attractive and repulsive states. An avoided crossing appears, leading to a purely long-range well connected to the 2^3S_1–2^3P_0 asymptote

of very precise molecular potentials for the interpretation of cold atom physics.

A new ab initio calculation of the potential has been made by Gadéa and co-workers [40,41]. In their 2002 paper [40], these authors had the primary objective of studying the robustness and reliability of the ab initio calculations and they revisited several points of the calculations of Stärck and Meyer, using various theoretical approaches and different basis states. In Fig. 3 of this paper, they summarized the calculated values of the scattering length a, showing a values as a function of the depth the $^5\Sigma_g^+$ molecular potential for their different theoretical approaches and they verified that the a values are extremely sensitive to even minor variations of the potential. In their 2004 paper [41], Gadéa and co-workers have developed hybrid potentials with a smooth connection of their ab initio calculation to an analytic expansion at long range: with these potentials, they have obtained the scattering length for the three possible isotopic combinations, including estimated error bars: for $^4\mathrm{He}^*$ atom pair, their result is $8.0 < a < 12.2$ nm [41] One can thus remark that a very precise measurement of a would be very helpful to test this very accurate interaction potential.

3.3 Measuring the interactions in the Bose Einstein condensate

With metastable helium, the first experimental determination of the scattering length a dates back from the Bose–Einstein condensation in 2001. The positive sign of a was confirmed by the possibility of obtaining a large stable condensed phase. In these experiments, the cold helium gas is first trapped in a magneto-optical trap, then transferred into a purely magnetic harmonic trap, where it is cooled one step further by the method of evaporative cooling, performed by radiofrequency induced spin flips. In the ENS experiment [38], the frequency is ramped down from 160 MHz to about 10 MHz in about 10 s. After evaporation, the trap is switched off and the cloud, released from the trap, is probed by absorption imaging on a CCD camera. At the end of the evaporation process, the temperature of the cloud drops down to a few microKelvin and the phase space density increases by six orders of magnitude. A narrow structure appears on the absorption image, which is identified as the Bose–Einstein condensate. The spatial distribution of the absorption picture is fitted with an inverted paraboloidal distribution for the condensed fraction, describing the equilibrium density profile within the harmonic trap in the Thomas-Fermi limit [44]. The strongest evidence for the presence of a condensate is the evolution of the shape of this structure when the cloud evolves in a time-of-flight measurement after that the trap is turned off. The aspect ratio of the cloud, or the anisotropy between the axial and radial directions, evolves in time during the expansion as a consequence of the mean-field interactions between the particles in the condensate. The interaction strength can thus be deduced from changes of ellipticity of the cloud as a function of the expansion time : the anisotropy increases and undergoes an inversion. Using the formalism of [44], one deduces from this a value for the chemical potential μ, from which one derives a value for the product aN, where N is the number of atoms in the condensed phase. One obtains a value for a provided N is properly evaluated. In [45] one finds the value $a = (16\pm8)$nm, in which the error is mostly due to the uncertainty on the number of atoms. In the BEC experiment of the Orsay group, which succeeded at the same time in 2001 [37], a value of $a = 20 \pm 10$nm was also derived from the properties of the condensate, detected through its expansion, as measured on a micro-channel plate.

3.4 Measuring elastic collision rates in the ultracold helium gas

One can also think of deriving the s-wave scattering length a from direct measurement of the elastic scattering collisions in the low temperature domain. A study of the evaporative cooling kinetics is a possible method which was theoretically developed by Luiten et al. [4]. It was adapted to the case of metastable helium in [46], by including the dependence of the elastic scattering cross section with the collision energy. They applied this modified theory to their experimental results, which cover a temperature range from 1.5 mK down to about 20 μK, an order of magnitude above condensation and thus obtained the following value: $a = 10 \pm 5$ nm. The uncertainty was due to several experimental factors such as the calibration of the atom detector or the temperature measurement.

An alternative method to measure elastic scattering cross sections was used by Leduc et al. [47], who studied collective excitations in the ultracold gas of metastable helium confined in a harmonic magnetic trap just above the BEC transition. The lowest monopole–quadrupole $m = 0$ modes of excitation were generated and the frequency and damping of the oscillations were measured as a function for decreasing temperatures, meaning increasing elastic collision rates. The dynamical behavior of the dilute gas can be described by the Boltzman equation. In this case two extreme situations can occur: the hydrodynamic regime, where the mean free path between colliding particles is small compared to the dimensions of the cloud; or the collisionless regime where the motion is described by the sum of single particle Hamiltonian. In both cases, the system shows well defined oscillations resulting from the external confinement, for which the frequency and the damping have been calculated, assuming a classical gas confined in an harmonic trap [48]. The comparison between experimental results and theory shows that when ramping the temperature down, one first explores the collisionless regime and then enters the hydrodynamic regime [49]. However no precise value could be derived for the collision rates, due to uncertainties regarding the number of metastable helium atoms, as well as to the unexpected departure from the runaway regime when reaching the condensation critical temperature. One should note that this method has been successfully applied in Walraven's group to the case of a thick cloud of rubidium atoms, for which the hydrodynamic regime was fully reached and the agreement of the derived collision rates in very good agreement with the already well known value of the scattering length (C. Buggle, private communication).

3.5 Getting the scattering length through inelastic collisions

Aspect's group developed a significantly different method to derive the scattering length of the ultracold metastable helium gas. They used the unique feature of metastable helium, which is the spontaneous Penning ionization in the sample as mentioned above. Their detection scheme is based on a micro-channel plate [37] which can either detect the positive ions produced by the inelastic two-body and three-body Penning collisions, or detect the metastable atoms, which loose their internal energy and produce electrons at the micro-channel plate. Two situations are studied: first, the pure BEC, for which the expansion by time-of-flight gives a relation between a, N the number of atoms, and μ the chemical potential; second, the thermal cloud at the critical temperature T_c for BEC condensation, which is simply related to N. As the atomic cloud is cooled through the phase transition, the ion rate presents a sudden increase at condensation: this provides an empirical determination of the transition. The corresponding value of T_c is deduced from time-of-flight signals obtained close to the transition with the atoms falling on the micro-channel plate. Finally the authors record the ion rate as a function of T_c, which they can fit with several inelastic collision parameters as well as with the elastic scattering length a. In short, combining the two experiments allows them to derive the value of a without needing the absolute calibration of the number of atoms N, which is the main source of uncertainty in all the previously described experiments. Their carefully derived a value is $a = 11.3^{+2.5}_{-1.0}$ nm [50], which is the most precise experimental value obtained so far.

3.6 Photoassociation and purely long range helium dimers

Photoassociation experiments in ultracold metastable helium were first undertaken with magneto-optical traps by laser cooling groups in the Netherlands [51]. The method was then used by the ENS group at temperatures much lower when studying the gas in a magnetic trap close to the BEC transition. This work is still in progress. The goal is to measure the position of the $v = 14$ vibrational level in the $^5\Sigma_g^+$ potential (see Fig. 4). The application of standard techniques to locate the highest vibrational level is not straightforward in this case: the situation is complicated by the autoionization of metastable helium dimers, which occurs at short internuclear distances. Only dimers in pure quintet spin configuration at short range are likely to avoid autoionization and sustain well resolved resonances. Indeed a few long-lived vibrational levels have recently been observed in molecular states close to the 2^3S_1–2^3P_2 transition (D_2), which might be helpful as intermediate levels in future two-laser photoassociation spectroscopy.

An interesting alternative was offered by the vibrational levels in the purely long range 0_u^+ potential below the 2^3S_1–2^3P_0 transition (D_0) line. Their positions were very precisely measured by Léonard et al. with a beam delivered by a diode laser amplified by a fibre amplifier, tuned close to the 2^3S–2^3P transition at 1,083 nm. They were also calculated with great precision and the agreement is excellent [45], showing clear evidence for measurable retardation effects in the electromagnetic interaction between the two atoms of the molecule. It was possible to calculate the positions of the

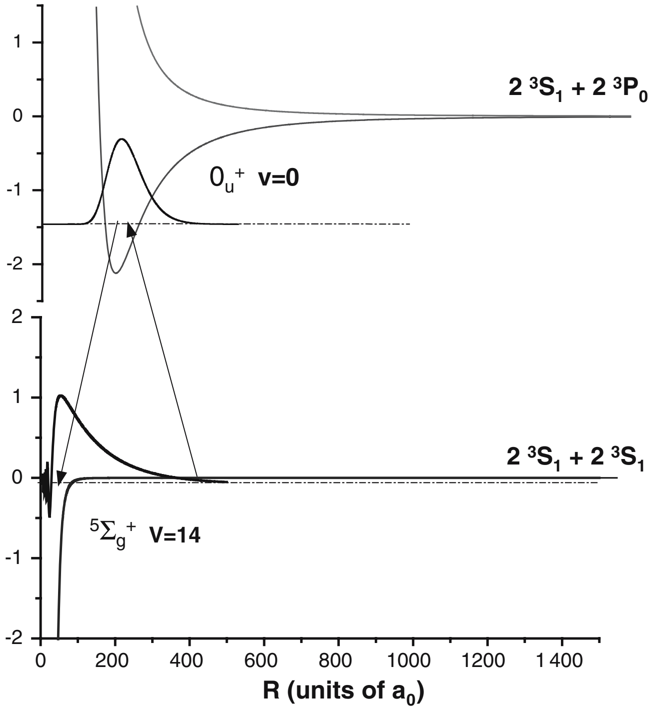

Fig. 4 Schematic of one and two-photon photoassociation experiments with helium atoms. Energies on the vertical axis are in gigahertz. A free pair of atoms in the $^2S - ^2S$ asymptote is excited with laser (1) to an intermediate molecular level of the $^2S - ^2P$ asymptote. Here, this molecular level is the $v = 0$ vibrational level of the purely long range 0_u^+ state. This allows to record one-photon photoassociation spectra. If one adds a second photon (2), it may stimulate the decay of the intermediate molecular state into the highest vibrational level ($v = 14$) of the $^5\Sigma_g^+$ state. Measuring the detuning between lasers (1) and (2) will give a very precise value of the binding energy of this vibrational level, from which the atom–atom scattering length in the $^5\Sigma_g^+$ state can be deduced very accurately

levels using a long-range Hamiltonian only incorporating the fine structure terms and the dipole–dipole interaction term in C_3/r^3 (corrected for retardation effects). Figure 3 illustrates the physical origin of the purely long-range 0_u^+ state. The joint effect of the dipole–dipole interaction and of the fine structure coupling leads to the appearance of an avoided crossing, which results in a purely-long range potential connected to the 2^3S_1–2^3P_0 asymptote. One notes that graph b) in Fig. 3 is only an intermediate step of calculation with no exact physical meaning, as the neglected coupling terms between attractive and repulsive states are not negligible. For such giant dimers, the inner turning point lies at such long range (150 a_0) that the short range autoionization process are fully inhibited.

3.7 Two-photon and single-photon photoassociation spectroscopy in helium

The search for the two-photon signal with two lasers through one vibrational level of the 0_u^+ state is in progress at ENS. The method is illustrated in Fig. 4. Despite their long range location, the wave functions of these excited vibrational levels have been estimated to have a sufficient Franck–Condon overlap with the wave function of highest vibrational level of the ground state potential $^5\Sigma_g^+$. In [52], numerical results are given for the amplitude and width of the expected spectra corresponding to the case of "frustrated photoassociation" with two lasers. Laser (1) is on resonance with the intermediate molecular state, causing an appreciable drop in the number of atoms in the trap. The frequency of laser (2) is scanned across the resonance between the two molecular states (see Fig. 4). At high enough intensity, when at resonance, laser (2) induces the upper bound state to undergo an Autler-Townes splitting [53] as described in the dressed-level picture. Consequently laser (1) is brought out of resonance and there is a recovery of the atomic density. An alternative method is the stimulated Raman two-photon spectroscopy, which is expected to provide very narrow lines with a width limited only by the lifetime of the level in the ground state. If a two-photon signal can be observed, a very precise value of a is expected, as was observed in the case of rubidium [29].

Alternative but less precise measurements deal with single-photon photoassociation. One can study the absolute photoassociation rate coefficients for the free-bound transition and deduce the Frank-Condon factors, which in turn can be calculated with a formalism which incorporates the value of the scattering length a. The comparison between Franck–Condon factors of different vibrational levels in the same excited molecular potential is likely to provide a value of a eliminating the systematic error related to the laser intensity calibration. Similarly one can also study the intensity shift of the photoassociation line, for which the theory is developed in several articles of Julienne and co-workers [54,55] and some experimental verifications are provided for alkali atoms [56]. Such experiments are currently on the way at ENS for a metastable helium gas close to BEC, using the $v = 0$ and $v = 1$ vibrational levels of the 0_u^+ state close to the D_0 transition. The theory includes the coupling of the involved levels to all the other levels nearby, in particular the continuum associated with the initial pair of free atoms. Preliminary results on the sign of the shift, constantly to the red of the transitions, tend to indicate an upper value for a (M. Portier, private communication). Quantitative results for a are expected soon.

3.8 Prospects for changing the interactions with optical Feshbach resonances

There was a proposal to modify the mean interaction strength between ultracold atoms by an appropriately detuned laser [57]. The requested laser intensities are quite large. Although great care must be taken to minimize scattering losses induced by the laser, some ranges of intensity and detuning can be found for a given experimental situation. Bohn and Julienne [58] have derived useful results concerning the modification of the scattering lengths by far off-resonant light.

A recent experiment by Grimm and co-workers demonstrates the possibility of tuning the scattering length of rubidium over a wide range, using such an optically induced Feshbach resonance [59].

This method is appealing in the case of metastable helium, at least with the ^{4}He isotope which has no hyperfine structure, because, in this case, there are no magnetic field induced Feshbach resonances. Prospects for substantial changes of a induced by light are analysed in a recent paper by Koelemeij and one of us [52]. Modifications of a to very high values as well as to vanishing or even negative values, is anticipated for experimentally realistic conditions, although the magnitude of the optical Feshbach resonance depends strongly on the exact value of a. To avoid substantial losses and heating of the trapped atoms, one may apply the laser beam only for a short duration.

4 Conclusion

Our goal was not to make a review of all the molecular data deduced from cold atom experiments but to show that the interpretation of the new information obtained through ultracold atom experiments requires very high quality molecular information, which can be given by traditional molecular high accuracy spectroscopy, but also requires good precision ab initio calculations of molecular potentials.

We have taken most of our examples from the studies with metastable helium dimers and we have briefly quoted some results obtained with alkali atoms. The experiments are numerous and the list of atom pairs studied is expanding every year. We have not discussed specifically the formation of cold molecules: this field is rapidly expanding and many recent results are reviewed in reference [60] and the following papers in the same issue of European Physical journal D.

We hope that we have convinced the quantum chemists that their help is needed and that the collaboration with cold atom physicists could be very fruitful.

Acknowledgements We want to acknowledge the role of J. P. Malrieu in our research community. The research group devoted to theoretical quantum chemistry, which has developed around him in Toulouse, has played an important role also for the physics community and we have much benefited from our interactions with J. P. Malrieu.

References

1. Côté R, Jamieson MJ, Yan Z-C, Geum N, Jeung G-H, Dalgarno A (2000) Phys Rev Lett 84:2806
2. Gadéa FX, Leininger T, Dickinson AS (2001) Eur Phys J D 15:251
3. Ketterle W (1996) Evaporative cooling, in advances in atomic, molecular, and optical physics, vol 37. In: Bederson B, Walther H, (eds) Academic Press, New York
4. Luiten OJ, Reynolds MW, Walraven JTM (1996) Phys Rev A 53:381
5. Koelman JMVA, Stoof HTC, Verhaar BJ, Walraven JTM (1987) Phys Rev Lett 59:676
6. Gribakin GF, Flambaum VV (1993) Phys Rev A 48:546
7. Leroy RJ, Bernstein RB (1970) Chem Phys Lett 5:42
8. Leroy RJ, Bernstein RB (1970) J Chem Phys 52:3869
9. Stwalley WC (1970) Chem Phys Lett 6:241
10. Tiesinga E, Moerdjik AJ, Verhaar BJ, Stoof HTC (1992) Phys Rev A 46:R1167
11. Tiesinga E, Verhaar BJ, Stoof HTC (1993) Phys Rev A 47:4114
12. Kerman AJ, Chin C, Vuletic V, Chu S, Leo PJ, Williams CJ, Julienne PS (2001) C R Acad Sci Paris. Elsevier, Amsterdam, 2(iv):633
13. Pethick CJ, Smith H (2002) Bose-Einstein condensation in dilute gases. Cambridge University Press, Cambridge
14. Moerdjik AJ, Verhaar BJ, Nagtegaal TM (1996) Phys Rev A 53:4343
15. Marinescu R, You L (1998) Phys Rev Lett 81:4596
16. Fedichev PO, Kagan Yu, Shlyapnikov GV, Walraven JTM (1996) Phys Rev Lett 77:2913
17. Gallagher A, Pritchard DE (1989) Phys Rev Lett 63:957
18. Julienne PS, Vigué J (1991) Phys Rev A 44:4464
19. Krauss M, Stevens WJ (1985) J Chem Phys 82:3224
20. Gibble K, Chu S (1993) Phys Rev Lett 70:1771
21. Sortais Y, Bize S, Nicolas C, Clairon A, Salomon C, Williams C (2000) Phys Rev Lett 85:3117
22. Wüest A, Merkt F (2004) J Chem Phys 120:638
23. Knöckel H, Johr T, Richter H, Tiemann E (1991) Chem Phys 152:399
24. Cline RA, Miller JD, Heinzen DJ (1994) Phys Rev Lett 73:632
25. Stwalley WC, Huang Y-H, Pichler G (1978) Phys Rev Lett 41:1164
26. McAlexander WI, Abraham ERI, Hulet RG (1996) Phys Rev A 54:R5
27. Jones KM, Julienne PS, Lett PD, Philipps WD, Tiesinga E, Williams CJ (1996) Europhys Lett 35:85
28. Côté R, Dalgarno A, Sun Y, Hulet RG (1995) Phys Rev Lett 74:3581
29. Wynar R, Freeland RS, Han DJ, Ryu C, Heinzen DJ (2000) Science 287:1016
30. Stwalley WC, Wang H (1999) J Mol Spectrosc 195:194
31. Weiner J, Bagnato VS, Zilio S, Julienne PS (1999) Rev Mod Phys 71:1
32. Masnou-Seeuws F, Pillet P (2001) Adv At Mol Opt Phys 47:53
33. Mastwilk HC, Thomsen JW, van der Straten P, Niehaus A (1998) Phys Rev Lett 80:5516
34. Tol PJJ, Herschbach N, Hessels EA, Hogervorst W, Vassen W (1999) Phys Rev A 61:R761
35. Shlyapnikov GV, Walraven JTM, Rahmanov UM, Reynolds MW (1994) Phys Rev Lett 73:3247
36. Venturi V, Whittingham IB, Leo PJ, Peach G (1999) Phys Rev A 60:4635
37. Robert A, Sirjean O, Browaeys A, Poupard J, Nowak S, Boiron D, Westbrook CI, Aspect A (2001) Sci Mag 292:463
38. Pereira Dos Santos F, Léonard J, Junmin W, Barrelet CJ, Perales F, Rasel E, Unnikrishnan CS, Leduc M, Cohen-Tannoudji C (2001) Phys Rev Lett 86:3459
39. Stärck J, Meyer W (1994) Chem Phys Lett 225:229
40. Gadéa FX, Leininger T, Dickinson AS (2002) J Chem Phys 117:7122
41. Dickinson AS, Gadéa FX, Leininger T (2004) J Phys B 37:587
42. Leo PJ, Venturi V, Whittingham IB, Babb JB (2001) Phys Rev A 64:042710
43. Yan ZC, Babb JF (1998) Phys Rev A 58:1247
44. Castin Y, Dum R (1996) Phys Rev Lett 77:5315
45. Léonard J, Walhout M, Mosk AP, Mueller T, Leduc M, Cohen-Tannoudji C (2003) Phys Rev Lett 91:073203
46. Tol PJJ, Hogervost W, Vassen W (2004) Phys Rev A 70:013404
47. Leduc M, Léonard J, Pereira dos Santos F, Jahier E, Schwartz S, Cohen-Tannoudji C (2002) Acta Phys Polonica B 33:2213
48. Guéry-Odelin D, Zambelli F, Dalibard J, Stringari S (1999) Phys Rev A 60:4851
49. Pitaevskii L, Stringari S (2003) Bose–Einstein condensation. Oxford University Press, Oxford
50. Seidelin S, Viana Gomes J, Hoppeler R, Sirjean O, Boiron D, Aspect A, Westbrook CI (2004) Phys Rev Lett 93:090409

51. Herschbach N, Tol PJJ, Vassen W, Hogervorst W, Woestenenk G, Thomsen JW, van der Straten P, Niehaus A (2000) Phys Rev Lett 84:1874
52. Koelemeij JC, Leduc M (2004) Eur Phys J D 31:263
53. Autler AH, Townes CH (1955) Phys Rev 100:703
54. Bohn JL, Julienne PS (1999) Phys Rev A 60:414
55. Simoni A, Julienne PS, Tiesinga E, Williams CJ (2002) Phys Rev A 66:063406
56. Prodan ID, Pichler M, Junker M, Hulet RG, Bohn JL (2003) Phys Rev Lett 91:080402
57. Fedichev PO, Reynolds MW, Rahmanov UM, Shlyapnikov GV (1996) Phys Rev A 53:1447
58. Bohn JL, Julienne PS (1997) Phys Rev A 56:1486
59. Theis M, Thalhammer G, Winkler K, Hellwig M, Ruff G, Grimm R, Hecker Denschlag J (2004) Phys Rev Lett 93:123001
60. Doyle J, Friedrich B, Krems RV, Masnou-Seeuws F (2004) Eur Phys J D 31:149